

<sup>63</sup>E. J. Johnson, in *Proceedings of the Ninth International Conference on the Physics of Semiconductors, Moscow, 1968* (Nauka, Leningrad, 1968), p. 276.

<sup>64</sup>P. Lawaetz and D. D. Sell (unpublished).

<sup>65</sup>W. Kohn and J. M. Luttinger, *Phys. Rev.* **98**, 915 (1955).

PHYSICAL REVIEW B

VOLUME 3, NUMBER 2

15 JANUARY 1971

## Extension of the Quasicubic Model to Ternary Chalcopyrite Crystals

J. E. Rowe

*Bell Telephone Laboratories, Murray Hill, New Jersey 07974*

and

J. L. Shay

*Bell Telephone Laboratories, Holmdel, New Jersey 07733*

(Received 19 June 1970)

A simple theoretical model is proposed to explain the recently observed valence-band structure of CdSnP<sub>2</sub> and similar chalcopyrite crystals. The valence bands of a chalcopyrite crystal are regarded as equivalent to those of a strained version of its binary analog. This model predicts the signs and magnitudes of the valence-band splittings observed in CdSnP<sub>2</sub> and ZnSiAs<sub>2</sub>. We show further that the quasicubic model explains quantitatively the unusual polarization dependences previously reported.

It has recently been reported<sup>1</sup> that the polarization selection rules governing the band-edge electroreflectance and photorelectance spectra of CdSnP<sub>2</sub> are opposite to those observed in wurtzite II-VI semiconductors and to theoretical predictions for similar chalcopyrite semiconductors. To explain this result, a new valence-band model was proposed<sup>1</sup> with the essential feature that the sign of the crystal-field splitting was opposite to that observed in wurtzite II-VI semiconductors. It is the purpose of this paper to provide a theoretical explanation for the proposed valence-band model, based on a very simple approximation to the crystal potential in chalcopyrite crystals. We show that the signs and magnitudes of the valence-band splittings in CdSnP<sub>2</sub> and ZnSiAs<sub>2</sub> (the only crystals for which electroreflectance data are available) can be predicted from the known properties of the binary analogs of these materials (e.g., InP is the binary analog of CdSnP<sub>2</sub>). We further show that the quasicubic model, developed by Hopfield<sup>2</sup> to explain properties of wurtzite crystals, can also be applied to chalcopyrite crystals with the result that the unusual polarization dependences observed experimentally can be explained quantitatively.

The valence-band model previously proposed<sup>1</sup> to explain the electroreflectance and photorelectance spectra of CdSnP<sub>2</sub> is shown in Fig. 1. The triply degenerate  $\Gamma_{15}$  in zinc blende is split in chalcopyrite such that the nondegenerate level  $\Gamma_4$  lies above the doubly degenerate  $\Gamma_5$ , just opposite to the ordering observed in wurtzite semiconductors. The doubly degenerate state is then split by spin-

orbit interaction. Hopfield's<sup>2</sup> quasicubic model regards the wurtzite crystal-field splitting as equivalent to the splitting produced by a trigonal uniaxial stress applied to a zinc-blende crystal. The strain

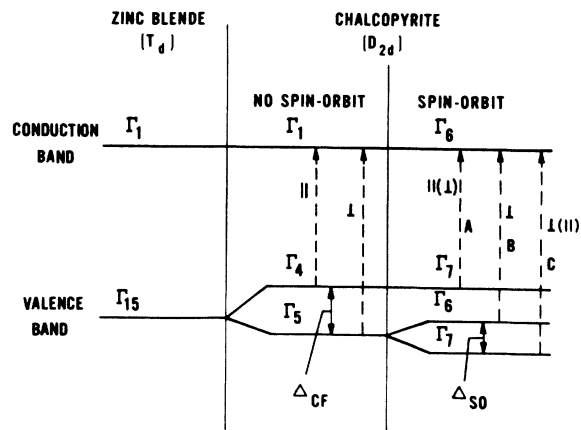


FIG. 1. Band structure and selection rules at  $k = [000]$  in zinc blende and chalcopyrite for light polarized relative to the optic axis. A, B, and C refer to the three peaks observed in electroreflectance spectra (Refs. 1 and 6). For the polarizations shown in parentheses, the transitions are allowed group theoretically but will be observed only to the extent that spin-orbit coupling mixes the unperturbed wave functions. For a finite  $\Delta_{CF}$  and  $\Delta_{SO}$ , the valence-band splittings must be determined using Eq. (1). For example, the separation of the  $\Gamma_7$  and  $\Gamma_6$  levels will be equal to  $\Delta_{SO}$  only in the limit that  $\Delta_{SO} \gg \Delta_{CF}$  and will be equal to  $(\frac{2}{3}) \Delta_{SO}$  in the limit that  $\Delta_{SO} \ll \Delta_{CF}$ .

Hamiltonian<sup>3,4</sup> is formally the same for both the trigonal distortion appropriate to wurtzite and the tetragonal distortion appropriate to chalcopyrite. Hence we can use the quasicubic model in both cases. The crystal-field splitting  $\Delta_{cf}$  and spin-orbit splitting  $\Delta_{so}$  parameters of the quasicubic model are determined from the observed valence-band splittings. Within this model, the energies of the  $\Gamma_7$  levels relative to the  $\Gamma_6$  level (see Fig. 1) are given by<sup>5</sup>

$$E_{1,2} = +\frac{1}{2}(\Delta_{so} + \Delta_{cf}) \pm \frac{1}{2}[(\Delta_{so} + \Delta_{cf})^2 - \frac{8}{3}\Delta_{so}\Delta_{cf}]^{1/2}. \quad (1)$$

Applying Eq. (1) to experimental data for  $\text{CdSnP}_2$ <sup>1</sup> and  $\text{ZnSiAs}_2$ <sup>6</sup> presented elsewhere, we determine the experimental values shown in Table I. Although the  $\Gamma_7 \rightarrow \Gamma_6$  transitions in Fig. 1 are allowed in both polarizations, it was observed both in  $\text{CdSnP}_2$ <sup>1</sup> and in  $\text{ZnSiAs}_2$ <sup>6</sup> that the lowest-energy transition (peak A) was strongly polarized  $E \parallel Z$ . We now present a simple model for the crystal potential in chalcopyrite which quantitatively explains this unusual polarization dependence as well as the observed splittings summarized in Table I.

Although the atomic positions in chalcopyrite are almost identical to those in zinc blende, there are three contributions to the noncubic crystal potential: (i) The ordering of the metal cations relative to one another is such that the unit cell is doubled along the optic axis; (ii) the anions are not located at  $(\frac{1}{4}, \frac{1}{4}, \frac{1}{4})$ , etc., positions, but are slightly distorted; and (iii) the chalcopyrite lattice is slightly compressed along the Z axis. We find that this compression along the optic axis dominates the other two noncubic potentials in determining the ordering of the valence bands in both  $\text{CdSnP}_2$  and  $\text{ZnSiAs}_2$ . The effects of the first two contributions have been calculated for  $\text{ZnSiAs}_2$ <sup>7</sup> and produce a splitting having the opposite sign and a magnitude  $\sim 30\%$  of the compressional splitting. Thus we expect the present model to slightly overestimate the crystal-field splittings (see Table I).

Insofar as the ordering of the valence bands is concerned, the chalcopyrite lattice can be regarded as a strained version of its binary analog. In other words, we assume that the valence-band structure of  $\text{CdSnP}_2$  is equivalent to that which would occur

TABLE I. Comparison of experimental results and theoretical predictions of the quasicubic model for the valence-band structure of  $\text{CdSnP}_2$  and  $\text{ZnSiAs}_2$ .

		$\Delta_{so}$ (eV)	$\Delta_{cf}$ (eV)	$I_{\parallel}/I_{\perp}$		
				A	B	C
$\text{CdSnP}_2$	Experiment <sup>a</sup>	0.10	-0.10	$\geq 20$	$\sim 0.2$	$\sim 0.1$
	Theory	0.11	-0.12	20	0	0.3
$\text{ZnSiAs}_2$	Experiment <sup>b</sup>	0.28	-0.13	9	$\sim 0$	$\sim 0.5$
	Theory	0.31	-0.16	8.5	0	0.5

<sup>a</sup>Reference 1.

<sup>b</sup>Reference 6.

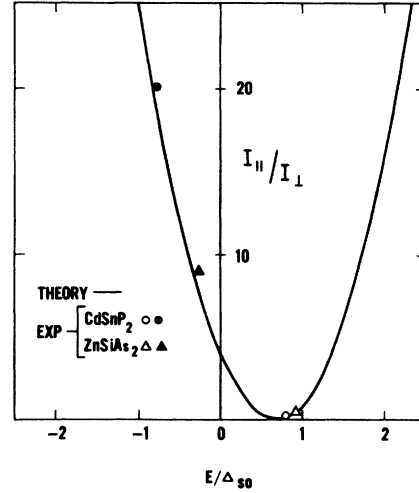


FIG. 2. Ratio of the strengths of transitions from a given  $\Gamma_7$  valence band to the  $\Gamma_6$  conduction band for light polarized, respectively, parallel or perpendicular to the optic axis. The solid line is the theoretical result of the quasicubic model from Eq. (2). The experimental points are taken from the A (solid circle, solid triangle) and C (open circle, open triangle) peaks of electroreflectance and photorefectance data.  $E$  is the energy of a  $\Gamma_7$  valence-band state relative to the  $\Gamma_6$  level, and  $\Delta_{so}$  is the spin-orbit splitting parameter.

in InP, could one strain InP sufficiently to produce the observed lattice constants of  $\text{CdSnP}_2$ . Naturally this model will be inadequate to explain phenomena which become allowed in chalcopyrite due to the doubling of the unit cell along the optic axis. In this approximation, the spin-orbit splitting  $\Delta_{so}$  predicted for  $\text{CdSnP}_2$  would be the value measured in InP,<sup>8</sup>  $\Delta_0$ . Similarly for  $\text{ZnSiAs}_2$ ,  $\Delta_{so}$  would be equal to the average of the  $\Delta_0$  values measured in GaAs<sup>8</sup> and AlAs. Since  $\Delta_0$  has not been measured for AlAs, we have used Herman's<sup>9</sup> theoretical value. Our theoretical values for  $\Delta_{so}$  predicted for the ternaries are shown in Table I and are in very good agreement with the experimental results.

It has been well established experimentally<sup>4,10,11</sup> that uniaxial compression of a cubic material splits the valence bands, producing an ordering of the energy levels in agreement with the  $\Gamma_4$  and  $\Gamma_5$  levels in Fig. 1. Using the known deformation potential describing this splitting in InP,<sup>11</sup> and the lattice constants of  $\text{CdSnP}_2$ ,<sup>12</sup> we predict a crystal-field splitting of  $-0.12$  eV for  $\text{CdSnP}_2$ . Similarly, we predict a crystal-field splitting of  $-0.16$  eV for  $\text{ZnSiAs}_2$  using only the deformation potential for GaAs,<sup>11</sup> since it is not available for AlAs. It can be seen in Table I that both theoretical values are very close to the experimental values. From the agreement between theory and experiment shown in Table I we conclude that the valence-band struc-

tures of both crystals are essentially the same as would occur in strained versions of their binary analogs.<sup>7</sup>

We mentioned earlier that the model in Fig. 1 was originally proposed<sup>1</sup> to explain the experimental observation that the lowest-energy  $\Gamma_7-\Gamma_6$  transition (peak A) was strongly polarized  $E \parallel Z$  in CdSnP<sub>2</sub>. It is at first surprising that the A peak is polarized  $E \parallel Z$ , since we see on the right-hand side of Fig. 1 that all transitions are either polarized  $E \perp Z$  or are allowed for both polarizations. This apparent anomaly is readily explained by the quasicubic model, and is in fact the principal success of the theory. For this model the ratio of the strengths of transi-

tions from a given  $\Gamma_7$  valence band to the  $\Gamma_6$  conduction band for light polarized, respectively, parallel or perpendicular to the optic axis is given by

$$I_{\parallel}/I_{\perp} = (2 - 3E/\Delta_{so})^2, \quad (2)$$

where  $E$  is given by Eq. (1). For the A peak in CdSnP<sub>2</sub>,  $E = -0.08$  eV,  $\Delta_{so} = 0.10$  eV, and Eq. (2) predicts that  $I_{\parallel}/I_{\perp} = 20$  in good agreement with experiment.<sup>1</sup> Equation (2) is shown as the solid line in Fig. 2, and the points represent the experimental intensity ratios for the A and C peaks of CdSnP<sub>2</sub><sup>1</sup> and ZnSiAs<sub>2</sub>.<sup>6</sup> The quasicubic model quantitatively explains the observed polarization dependences.

<sup>1</sup>J. L. Shay, E. Buehler, and J. H. Wernick, Phys. Rev. Letters **24**, 1301 (1970).

<sup>2</sup>J. J. Hopfield, J. Phys. Chem. Solids **15**, 97 (1960). It has been claimed in the literature that Hopfield's quasicubic model is a crude approximation which neglects the tetrahedral symmetry of the unstrained cubic crystal. This is not correct since the  $\Gamma_{15}$  representation of the  $T_d$  group is in one-to-one correspondence with the  $L = 1$  representation of the full-rotation group. Within the  $\Gamma_{15}$  subspace of states both symmetries are equivalent.

<sup>3</sup>E. O. Kane, Phys. Rev. **178**, 1368 (1969).

<sup>4</sup>F. H. Pollak and M. Cardona, Phys. Rev. **172**, 816 (1968).

<sup>5</sup>The sign convention is the same as in Ref. 2.

<sup>6</sup>J. L. Shay, E. Buehler, and J. H. Wernick (unpublished).

<sup>7</sup>A. S. Poplavnoi, Izvest. Vuz. Fiz. (USSR) **11**, 142 (1968). In this work it is shown that the first two non-cubic potentials enumerated earlier produced a positive  $\Delta_{ct}$  of  $\sim 0.05$  eV in ZnSiAs<sub>2</sub>. This positive contribution to  $\Delta_{ct}$  improves the already good agreement between theory and experiment in Table I.

<sup>8</sup>M. Cardona, K. L. Shaklee, and F. H. Pollak, Phys. Rev. **154**, 696 (1967).

<sup>9</sup>F. Herman, C. D. Kuglin, K. F. Cuff, and R. L. Kortum, Phys. Rev. Letters **11**, 541 (1963).

<sup>10</sup>D. G. Thomas, J. Appl. Phys. **32S**, 2298 (1961).

<sup>11</sup>A. Gavini and M. Cardona, Phys. Rev. B **1**, 672 (1970).

<sup>12</sup>A. S. Borshchevskii, N. A. Goryunova, F. T. Kesamanly, and D. N. Nasledov, Phys. Status Solidi **21**, 9 (1967).

## Microwave Phonon Attenuation Measurements in *n*-Type Silicon<sup>†</sup>

Michel Dutoit\*

Department of Electrical Engineering, Washington University, St. Louis, Missouri 63130  
(Received 17 June 1970)

Microwave phonon attenuation at 9.3 GHz in *n*-type silicon has been measured between 2 and 100 K. The excess attenuation observed in impure samples is attributed to conduction electrons. The intervalley relaxation time is determined from these results for Sb- and As-doped silicon with impurity concentration between  $3 \times 10^{17}$  and  $2 \times 10^{19}$  cm<sup>-3</sup>. A large excess attenuation, not accounted for by any existing theories, is observed at low temperatures in nondegenerate samples. The discrepancy between experiment and theory is thought to arise from electrons in impurity states. It is suggested that hopping conduction may explain our results at low temperatures. No specific influence of impurity band formation on attenuation is found experimentally.

### I. INTRODUCTION

In the last decade, high-frequency ultrasonic techniques have become increasingly useful for studies in solid-state physics.<sup>1,2</sup> One phenomenon that can be investigated in this manner is intervalley scattering in many-valley semiconductors. In conventional transport experiments, the effect of intervalley scattering appears only as a small perturba-

tion on the background of intravalley scattering, which has a much higher probability; thus, the intervalley contribution is difficult to evaluate. Conversely, ultrasonic attenuation in doped material strongly depends on the intervalley relaxation time. The strain-induced variation of their energy causes the electrons to undergo transitions to lower states. This relaxation takes a finite time and, therefore, some power will be lost by the ultrasonic wave to